Virus Genes (2019) 55:630–642
https://doi.org/10.1007/s11262-019-01683-x

ORIGINAL PAPER

Upregulated expression of the antioxidant sestrin 2 identified by transcriptomic analysis of Japanese encephalitis virus-infected SH-SY5Y neuroblastoma cells

Michael Carr[1,2] · Gabriel Gonzalez[3] · Axel Martinelli[1] · Christida E. Wastika[4] · Kimihito Ito[3] · Yasuko Orba[4] · Michihito Sasaki[4] · William W. Hall[1,2,5] · Hirofumi Sawa[1,4,5]

Received: 18 February 2019 / Accepted: 2 July 2019 / Published online: 10 July 2019

Abstract

Japanese encephalitis virus (JEV) exerts a profound burden of viral encephalitis. We have investigated the differentially expressed transcripts in the neuronal transcriptome during JEV infection by RNA sequencing (RNA-Seq) of virus-infected SH-SY5Y human neuroblastoma cells. Gene ontology analysis revealed significant enrichment from two main pathways: endoplasmic reticulum (ER)-nucleus signaling (*P* value: 5.75E−18; false discovery rate [FDR] 3.11E−15) and the ER unfolded protein response (*P* value: 7.58E−18; FDR 3.11E−15). qPCR validation showed significant upregulation and differential expression ($P < 0.01$) of ER stress-signaling transcripts (*SESN2*, *TRIB3*, *DDIT3*, *DDIT4*, *XBP1*, and *ATF4*) at 24 h post-infection for both low (LN) and high (HN) neurovirulence JEV strains. Immunoblot analysis following JEV infection of SH-SY5Y cells showed an increase in levels of SESN2 protein following JEV infection. Similarly, Zika virus (MR766) infection of SH-SY5Y showed a titer-dependent increase in ER stress-signaling transcripts; however, this was absent or diminished for *DDIT4* and *ATF4*, respectively, suggestive of differences in the induction of stress-response transcripts between flaviviruses. Interestingly, *SLC7A11* and *SLC3A2* mRNA were also both deregulated in JEV-infected SH-SY5Y cells and encode the two constituent subunits of the plasma membrane xCT amino acid antiporter that relieves oxidative stress by export of glutamate and import of cystine. Infection of SH-SY5Y and HEK293T cells by the JEV HN strain Sw/Mie/40/2004 lead to significant upregulation of the *SLC7A11* mRNA to levels comparable to *DDIT3*. Our findings suggest upregulation of antioxidants including SESN2 and, also, the xCT antiporter occurs to counteract the oxidative stress elicited by JEV infection.

Keywords Japanese encephalitis virus · Neuron · RNA-Seq · Sestrin · xCT antiporter

Introduction

Japanese encephalitis virus (JEV) is a pathogenic, mosquito-borne flavivirus with mortality of 30% and debilitating neurological symptoms in up to 50% of convalescent cases [1–4]. Although there are effective vaccines, JEV remains the principal pathogen associated with Asian cases of viral

Edited by Hartmut Hengel.

Electronic supplementary material The online version of this article (https://doi.org/10.1007/s11262-019-01683-x) contains supplementary material, which is available to authorized users.

✉ Michael Carr
michael.carr@ucd.ie

[1] Global Station for Zoonosis Control, Global Institution for Collaborative Research and Education (GI-CoRE), Hokkaido University, N20, W10, Kita-ku, Sapporo 001-0020, Japan

[2] National Virus Reference Laboratory, School of Medicine, University College Dublin, Belfield, Dublin 4, Ireland

[3] Division of Bioinformatics, Research Center for Zoonosis Control, Hokkaido University, N20, W10, Kita-ku, Sapporo 001-0020, Japan

[4] Division of Molecular Pathobiology, Research Center for Zoonosis Control, Hokkaido University, N20, W10, Kita-ku, Sapporo 001-0020, Japan

[5] Global Virus Network, Baltimore, MD 21201, USA

encephalitis, with approximately 67 900 cases per annum in 24 countries with endemic disease [5]. The highest age-specific infection rates occur in younger age groups, where the disease is also more severe; 75% (ca. 51 000) of JEV cases occur in children 0–14 years old [5].

The innate immune response to viral infection is essential to limit viral replication of pathogens and to affect their elimination from host tissues. Based on findings of the mechanism of JEV neuropathogenesis in rhesus macaques, a model has been proposed for apoptosis of neurons and activation of glia and cytokine release as important steps in JEV-mediated neuronal death [6]. The macaque study corroborates that neurons are the principal targets of JEV, as has also been previously indicated by post-mortem human studies, where neurons in the cortex and brainstem were positive for viral antigen [7–9]. A cDNA microarray analysis of JEV-infected murine neuroblastoma cell lines identified significantly altered mRNA expression, including genes involved in host antiviral responses and apoptotic cell death [10]. Traditionally, neurons were thought of as immunologically quiescent, which may explain the paucity of JEV infection studies in human neuronal cells; however, there is growing evidence for effective neuronal antiviral responses [11–15].

Sestrins (SESNs) are highly conserved proteins and have been implicated in cellular protective responses to environmental stressors, including oxidative stress and DNA damage [16, 17]. SESNs serve to potentiate adenosine monophosphate-activated protein kinase (AMPK) and to inhibit signaling through the mechanistic target of rapamycin complex 1 (mTORC1) [18] that acts to regulate cellular growth and metabolism and maintain cellular and organismal homeostasis [19]. mTORC1 activation induces the increase in reactive oxygen species (ROS) by a number of distinct biological pathways, comprising the induction of endoplasmic reticulum (ER) stress, elevated anabolic biosynthesis and the inhibition of autophagy [20, 21]. Sestrin 2 (SESN2) is a leucine sensor and results in autophagy by activating AMPK and inhibiting mTORC1 in vitro when exposed to genotoxic stressors [22–24]. SESN2 depletion in murine culture leads to accumulation of ROS [16], whereas conversely, SESN2 overexpression is protective against a range of insults, such as, hypoxia, glucose deprivation or exposure to hydrogen peroxide [25], consistent with an antioxidant function. The antioxidant activity of SESN2 is attributed to cysteine sulfinic acid reductase activity, required to activate peroxiredoxins [16]. SESN2 has been shown to inhibit chronic activation of the NLRP3 inflammasome by clearance of injured mitochondria by inducing mitophagy of macrophages [26]. SESN2 knockout mice displayed defects in mitophagy leading to inflammasome hyperactivation and decreased survival rates in murine models of sepsis [26].

In the present study, we have employed RNA sequencing (RNA-Seq) [27] to generate a detailed transcriptomic analysis of the deregulated neuronal transcripts upon JEV infection. Following infection of SH-SY5Y human neuroblastoma cells with a high neurovirulence JEV strain, we identified significant upregulation of ER stress-signaling transcripts (*SESN2*, *TRIB3*, *DDIT3*, *DDIT4*, *XBP1*, and *ATF4*) and, also, of both the *SLC7A11* and *SLC3A2* mRNAs which encode the two constituent subunits of the xCT (system x_c^-) amino acid antiporter. These findings demonstrate that JEV neuronal infection in vitro leads to increased expression of antioxidant transcripts which may have implications for studies of flavivirus neuropathogenesis.

Materials and methods

Cell culture

Cells were cultured under 5% CO_2 at 37 °C in growth medium: the human SH-SY5Y neuroblastoma cell line (94030304, ECACC, HPA, UK) was propagated in Dulbecco's modified Eagle's medium (DMEM) F12 (D8062, Sigma) with 10% fetal calf serum (FCS); the human embryonic kidney cell line HEK293T (632180, Takara Bio, Shiga, Japan) was cultured in DMEM high glucose medium (D6429, Sigma) with 10% FCS; Vero cells were propagated in DMEM supplemented with 10% FCS.

Antibodies

Anti-SESN2 rabbit monoclonal (ab178518, Abcam) diluted 1:1000; anti-TRIB3 (B-2) diluted 1:1000 (sc-390242, Santa Cruz); anti-JEV NS3 rabbit polyclonal diluted 1:3000 (GTX125868, GeneTex); anti-JEV NS5 rabbit polyclonal diluted 1:20000 (GTX131359, GeneTex). β-actin was employed as a loading control and the direct anti-β-actin antibody conjugated to horseradish peroxidase (PM053-7, MBL) diluted 1:2000. All antibodies were diluted in Tris-buffered saline with 0.1% Tween 20 (TBST) buffer including 5% skimmed milk.

Plaque assays

Vero cells were plated in 6-well plates to produce confluent cell monolayers the following day and then infected by incubation with tenfold serial dilutions of C6/36-amplified JEV strains Sw/Mie/41/2002 and Sw/Mie/40/2004 [28] for 1 h with shaking at 37 °C and then overlaid with Eagle's medium containing 1% methylcellulose. When plaques became visible then cells were fixed with 10% buffered formalin then stained with 1% crystal violet before removal

of the overlay medium. Viral titers were calculated and expressed as plaque forming units (PFU)/ml.

RNA sequencing and analysis

Total RNA was extracted from SH-SY5Y cells grown in 6-well plates following mock infection or infection with a JEV HN strain (Sw/Mie/40/2004) 24 h post-infection (hpi) with a multiplicity of infection (MOI) of 25 with four biological replicates for each experimental condition employing TRIzol (Life Technologies), the Direct-zol RNA kit (Zymo Research) and DNaseI treatment (Thermo Fisher), according to the manufacturer's instructions. A total of 5 µg of total RNA was subjected to ribosomal RNA (rRNA) depletion using the Ribo-Zero Gold rRNA Removal Kit (Illumina). Post-depletion RNA quantity and quality was evaluated using the Agilent 2100 Bioanalyzer instrument with the Agilent RNA 6000 Pico Kit (Agilent Technologies). Library construction was performed employing the TruSeq Stranded Total RNA Library kit (Illumina), omitting the first poly(A) + RNA selection step by oligo(dT) beads, as rRNA-depleted RNA was employed, and then proceeding according to the manufacturer's protocol without further modifications. Library profiles were examined employing the DNA High Sensitivity LabChip kit on an Agilent Bioanalyzer. Libraries were sequenced on the NovaSeq 6000 platform (Illumina) with 150 base-length read chemistry in a paired-end mode. The raw data of sequence reads from this study have been submitted to the Sequence Read Archive (SRA) database (https://www.ncbi.nlm.nih.gov/sra) under accession number DRA007709. Kallisto v.0.44.0 (https://pachterlab.github.io/kallisto/about) was used to quantify abundance of transcripts in the replicates [29] with version GRCh38.p12/CDNA of the human reference genome. Subread v.3.8 (https://bioconductor.org/packages/release/bioc/html/Rsubread.html) [30] was used to align reads to genes in the human reference genome. EdgeR [31] and DESeq 2 [32] were used to perform the transcript expression analysis with the following thresholds to filter the results of deregulated transcripts with a false discovery rate (FDR) < 0.05 in EdgeR, and adjusted *P* value (padj) < 0.05 in DESeq 2.

Relative quantification by qPCR of neuronal transcripts in virus-infected cells

Two-step real-time PCR (qPCR) relative quantification normalized to endogenous controls was employed to determine mRNA levels for validation of differentially expressed genes (DEGs) identified by RNA-Seq. cDNA was generated from total RNA samples using the SuperScript VILO cDNA synthesis kit (Thermo Fisher) and incubated at 25 °C for 10 min, 50 °C for 50 min and 85 °C for 5 min. qPCR for SYBR green relative quantification of the ER stress-signaling transcripts (*SESN2*, *TRIB3*, *DDIT3*, *DDIT4*, *XBP1*, and *ATF4*) were prepared using the SYBR Premix Ex Taq II (Tli RNaseH Plus), ROX plus (Takara) normalized to the endogenous *U6* transcript. qPCR was performed on the StepOnePlus Real-Time PCR System (Applied Biosystems) with the following thermocycling conditions: 95 °C for 30 s; followed by 40 cycles at 95 °C for 5 s and 60 °C for 30 s and a melt curve analysis of 95 °C for 15 s, 60 °C for 1 min and 95 °C for 15 s. The relative mRNA transcript levels were measured from four biological replicates. The oligonucleotide primer pairs for each gene target are included in the Supplementary Table. For relative quantification of *SLC7A11* and *DDIT3*, inventoried TaqMan assays (Applied Biosystems) for *SLC7A11* (Cat. # 4331182), *DDIT3* (Cat. # 4331182) and *GAPDH* (Cat. # 4448489) were used. Real-time PCR for TaqMan relative quantification were prepared with the Thunderbird probe qPCR mix (Toyobo). qPCR was performed on the StepOnePlus Real-Time PCR System (Applied Biosystem) with the following thermocycling conditions: 95 °C for 1 min; followed by 40 cycles at 95 °C for 15 s and 60 °C for 1 min. Relative expression levels were calculated by the comparative cycle threshold (C_T) method and represented as relative quantification (RQ). The C_T values for the target gene were normalized to the C_T for endogenous controls in the same sample. RQ is defined as $2^{-\triangle\triangle C_T}$, where $\Delta\Delta C_T = \Delta C_T$ sample $- \Delta C_T$ calibrator.

Immunofluorescence

The JEV-infected and control uninfected HEK293T cells were fixed 24 hpi in 4% paraformaldehyde for 20 min. Cells were permeabilized in phosphate-buffered saline (PBS) containing 0.5% Triton-X-100 for 5 min then blocked for 30 min with Block Ace (Bio-Rad) prior to addition of rabbit anti-JEV hyperimmune serum (1/2000 dilution) [33] for 1 h then were cells washed 4 times in TBST. The immune complexes were visualized by incubation with a goat anti-rabbit IgG Alexa Fluor 488-conjugated secondary antibody (Invitrogen) and cell nuclei were counter-stained with 4,6-diamidino-2-phenylindole then finally washed 4 times in TBST. Fluorescent cells were visualized by confocal microscopy (Olympus IX73).

Immunoblotting

Cell monolayers were lysed in in lysis buffer [10 mM Tris–HCl (pH 7.5), 150 mM NaCl, 0.5 mM EDTA and 0.5% NP-40] for 10 min on ice then centrifuged at 20380×*g* for 10 min. Proteins were separated by sodium dodecyl sulfate-polyacrylamide electrophoresis (SDS-PAGE) and then transferred to polyvinylidene difluoride (PVDF) membranes (Bio-Rad) at 15 V for 1 h using a Bio-Rad Trans-blot instrument. The membrane was then blocked in TBST

buffer [50 mM Tris–HCl (pH 7.5); 150 mM NaCl; 0.05% Tween-20] containing 5% skimmed milk for 1 h. Membranes were then incubated with primary antibody for 1 h at room temperature, then washed three times with TBST. Secondary antibody incubation was with goat anti-rabbit or goat anti-mouse IgG-horseradish peroxidase (HRP) dependent on the primary antibody, each at 1:6000 dilution in TBST buffer. After washing three times with TBST buffer, the membrane was developed with enhanced chemiluminescence (ECL) substrate (Thermo Fisher) and the signal was detected by a BIO-RAD Fluorescent Imager.

Statistical analysis

Statistical analysis was performed by calculating the *P* value with two tailed *t* tests. A confidence level of 95% ($P < 0.05$) was considered statistically significant.

Results

RNA-sequencing transcriptomics identifies deregulation of SESN2 in JEV-infected SH-SY5Y neuroblastoma cells

Paired-end read 150 bp cDNA libraries were constructed from rRNA-depleted total RNA from mock and JEV HN (Sw/Mie/40/2004)-infected SH-SY5Y neuroblastoma cells at 24 hpi. The infection rate of JEV strain Sw/Mie/40/2004 in SH-SY5Y neuroblastoma cells at 24 hpi with increasing MOI (10, 25, 50, and 100) was assessed by immunofluorescence (Supplementary Fig. 1). The signal derived from an anti-JEV antibody was comparable at MOIs > 25; therefore, we performed the RNA-Seq analysis on RNA derived from SH-SY5Y cells infected with a MOI of 25 at 24 hpi to examine the early transcriptomic response to viral infection. Sequencing was performed to high depth on an Illumina NovaSeq 6000 platform generating 110 gigabases of data and approximately 40 M reads for each of four biological replicates for the infected and uninfected samples at 24 hpi. To assess the degree of variability between the mock- and JEV-infected biological replicates prior to analysis, raw data variance was assessed by principal components analysis (PCA) and a t-distributed Stochastic Neighbour Embedding (t-SNE) plots of "Control" (mock-infected SH-SY5Y cells) versus "Infected" (JEV strain Sw/Mie/40/2004-infected) SH-SY5Y neuroblastoma cells at 24 hpi was performed (Supplementary Fig. 2) which showed clear separation among different treatments and less variation among biological replicates. As a quality control of the experimental setting, we compared the coefficient of variation (CV) among replicates of the control and virus-infected cells (Supplementary Fig. 3). Analysis of normalized read counts per gene showed that 15,879 out of 20,512 genes (77.4%) have counts above zero in all the replicates and treatments. The CV for the control and infected replicates was < 0.5 in 94% and 96% of the genes, respectively. In addition, we assessed the biological coefficient of variation (BCV) with edgeR with values confirming as the counts per million (CPM) increases the expected BCV decreased. Also, the low common dispersion provides a high degree of confidence in the power of the present study to identify differentially expressed genes (DEGs).

To identify DEGs, we employed two separate statistical RNA-Seq analysis workflows, based on fragments per kilobase of transcript per million mapped reads (FPKM) values and read counts, employing two computational methodologies: edgeR and DEseq 2. By comparing the RNA-Seq results from mock and JEV HN (Sw/Mie/40/2004)-infected SH-SY5Y neuroblastoma cells, edgeR and DEseq 2 identified 299 and 352 DEGs, respectively, which have a *P* value < 0.05 after correction for multiple testing. We identified 201 DEGs in the intersection of both analyses, in which 164 genes are upregulated and 37 genes are downregulated (Supplementary Fig. 4). Gene ontology (GO) term analysis of differentially expressed gene transcripts identified significant enrichment of mRNAs derived from two main pathways following JEV infection: ER-nucleus signaling (*P* value 5.75E−18; FDR 3.11E−15) and the ER unfolded protein response (UPR) (*P* value 7.58E−18; FDR 3.11E−15) consistent with flavivirus replication within the ER (Table 1).

Heat maps of significantly up- and downregulated transcripts between mock and JEV-infected SH-SY5Y cells at 24 hpi are shown in Fig. 1a with four biological replicates for each experimental condition. We performed a gene set enrichment analysis to identify biological pathways that were significantly altered ($P < 0.05$). Several biological pathways related to protein processing in the ER, aminoacyl tRNA biosynthesis, antigen processing and presentation, HTLV-1 infection, spliceosome processing, estrogen signaling and prion diseases were found to be significantly upregulated in JEV-infected SH-SY5Y neuroblastoma cells (Fig. 1b). The most significantly affected pathway was protein processing in the ER in agreement with the GO term analysis. Figure 1c shows in red the significantly upregulated transcripts during ER protein processing which can be sub-divided into: (A) Proteins involved in recognition by ER luminal molecular chaperones involved in protein folding, such as HYOU1, HSPA5, HSP90B1, and DNAJC3 [34]; (B) Proteins associated with ER-associated degradation (ERAD): EDEM1 (ER degradation-enhancing alpha-mannosidase-like protein 1) which targets misfolded glycoproteins [35], ERP29 (ER resident protein 29) which plays a critical role in the processing and folding of secretory proteins within the ER [36], SSR2 (signal sequence receptor subunit beta) which binds calcium to the ER membrane and regulates retention of ER resident proteins and is required

Table 1 Gene ontology (GO) term analysis of the deregulated pathways following JEV HN high neurovirulence (Sw/Mie/40/2004)-infected SH-SY5Y cells 24 hpi

Deregulated biological pathway	Total	Expected	Hits	*P* value	FDR
Endoplasmic reticulum unfolded protein response	93	1.01	18	5.75E−18	3.11E−15
ER-nucleus signaling pathway	111	1.2	19	7.58E−18	3.11E−15
Homophilic cell adhesion	139	1.51	11	3.25E−07	8.89E−05
Positive regulation of hydrolase activity	497	5.39	18	7.42E−06	0.00152
Response to organic substance	2500	27.1	47	5.88E−05	0.00964
Neutral amino acid transport	23	0.25	4	1.00E−04	0.0137
Steroid biosynthetic process	183	1.99	9	0.000172	0.0202
Regulation of neuron apoptotic process	150	1.63	8	0.000229	0.0235
Positive regulation of transferase activity	510	5.53	15	0.000437	0.0398
ER to Golgi vesicle-mediated transport	62	0.673	5	0.000554	0.0423
Cellular response to stress	1620	17.6	32	0.000568	0.0423

FDR false discovery rate

for WNV pathogenicity [37], HSPA1A (heat shock 70 kDa protein 1A) whose overexpression has been associated with the amelioration of neurological disease [38] and HERPUD (homocysteine-responsive endoplasmic reticulum-resident ubiquitin-like domain member) which is involved in the unfolded protein response (UPR) and ERAD and, interestingly, has been found upregulated in the substantia nigra of Parkinson's disease (PD) patients [39]; and, finally, (C) Activation of UPR sensors. In higher eukaryotes, the UPR relies on three UPR sensors on the ER membrane which trigger signaling cascades: ERN1, EIF2AK3 (also known as PERK), and ATF6 (activating transcription factor-6α) [40]. In the JEV neuronal transcriptome, both the EIF2AK3 and ERN1 pathways appeared activated as we identified significantly upregulated ATF4 (activating transcription 4) in the former and XBP1 (X-box binding protein) in the latter. ATF4 and XBP1 are upstream of the nuclear localized DDIT3 (DNA damage inducible transcript 3) which plays a key role in cellular stress response and was the most significantly deregulated transcript between the mock and JEV-infected SH-SY5Y cells (Fig. 1a) in our analysis [41]. Taken together, these results indicate significant upregulation of molecular chaperones to facilitate protein folding and an induction of the ERAD and ER stress-signaling between the ER and the nucleus during the ER UPR following JEV infection of neuroblastoma cells.

SESN2 and *TRIB3* are significantly upregulated 24 h post-infection in JEV and ZIKV-infected SH-SY5Y cells

In order to validate the ER stress-signaling transcripts determined by RNA-Seq to be significantly upregulated following JEV infection of SH-SY5Y cells when compared with mock-infected control cells at 24 h, we performed relative quantification of the DEGs by qPCR. Consistent with the RNA-Seq and GO term analyses, the qPCR data showed significant differential expression ($P < 0.01$) of *SESN2*, *TRIB3*, *DDIT3*, *DDIT4*, *XBP1*, and *ATF4* at 0 hpi for both the HN strain (Sw/Mie/40/2004) employed in the RNA-Seq experiment and, also, the LN strain (Sw/Mie/41/2002) when compared to mock-infected cells at 24 h (Fig. 2a–f; [42]). At the earlier time point at 8 hpi, there was no significant differences in the relative mRNA levels of the ER stress-signaling transcripts between either of the JEV LN or HN-infected SH-SY5Y cells and mock-infected controls at 0 hpi. Immunoblot analysis of protein expression following JEV infection (at MOIs ≥ 10) of SH-SY5Y cells showed that there was an increase in levels of SESN2 protein at 24 hpi following JEV LN infection; however, there was no equivalent increase following JEV HN infection (Fig. 3), despite comparable protein levels of the viral NS3 and NS5 antigens and the endogenous β-actin controls. The increase of TRIB3 mRNA for both LN and HN JEV strains was not reflected in a corresponding increase in protein levels 24 hpi at any of the viral titers tested.

We next examined the corresponding ER stress-signaling transcripts 24 hpi following SH-SY5Y infection by the related flavivirus Zika (ZIKV strain MR766) (Fig. 4a–f). Interestingly, while a clear titer-dependent increase in expression of *DDIT3* and *XBP1* was seen following ZIKV infection, however, this was absent for *DDIT4* and *ATF4*. Notably, however, both *SESN2* and *TRIB3* were significantly deregulated at higher MOIs tested.

The xCT antiporter light chain subunit *SLC7A11* mRNA is deregulated in JEV-infected SH-SY5Y and HEK293 cells

SLC7A11 and *SLC3A2* (the light and heavy chain subunits of xCT) were the fourth and sixth most significantly DEGs, respectively, on the heat map in Fig. 1a and encode the two constituent subunits of the plasma membrane xCT antiporter (also known as system x_c^-), that exerts an antioxidant

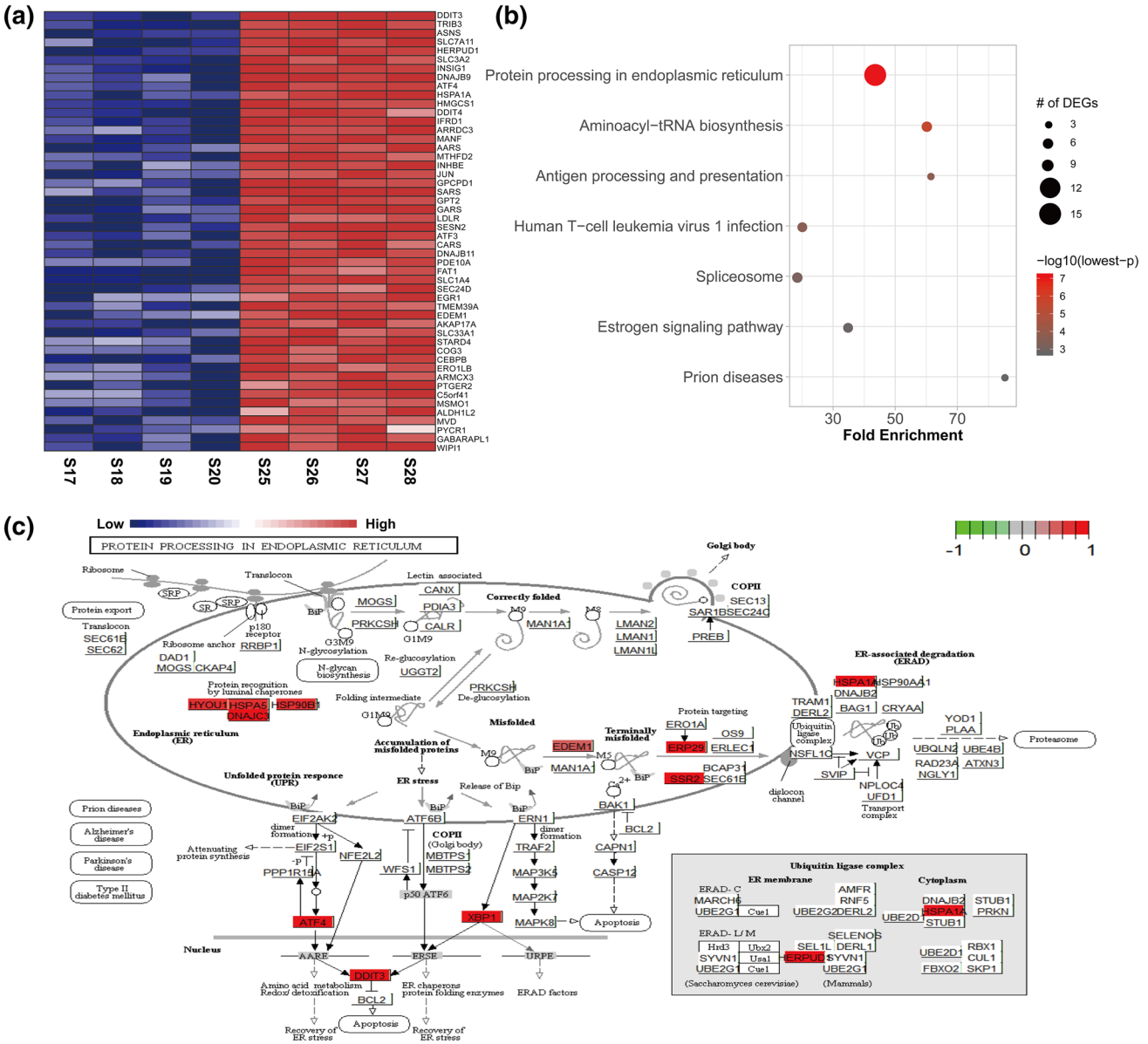

Fig. 1 JEV-infected neuronal transcriptome. **a** Heat map analysis of the JEV-infected neuronal transcriptome. The samples S17-S20 represent four biological replicates derived from mock-infected SH-SY5Y neuroblastoma cells and the samples S25-S28 represent four biological replicates derived from JEV high neurovirulence (Sw/Mie/40/2004)-infected (MOI 25) SH-SY5Y cells 24 hpi. The upper and bottom heat maps show the up- and downregulated genes in the infected cells, respectively. **b** Pathways inferred as enriched by deregulated genes. The size of the circles is proportional to the number of genes identified to be significantly deregulated and the color reflects the significance of the number of deregulated genes. The vertical axis shows the pathways in descending order by the number of deregulated genes and the horizontal axis represents the fold enrichment. **c** Pathway of protein processing in the endoplasmic reticulum with deregulated genes highlighted in color

function by exporting the amino acid glutamate to the extracellular milieu and imports the oxidized monomeric amino acid cystine [43]. Disruption of the xCT antiporter system enhances cell viability after glucose depletion, as glutamate conservation allows cells to maintain mitochondrial respiration [44]. SLC7A11 is the light chain of the xCT antiporter system and is the specific subunit of system x_c^-, whereas SLC3A2 (the heavy chain) is present in other amino acid transport systems. Therefore, we measured by qPCR the DEG *SLC7A11* mRNA transcripts relative to the endogenous control *GAPDH* and this is shown compared to the most significantly deregulated transcript *DDIT3* in Fig. 5. In agreement with the RNA-Seq data, SH-SY5Y infection by the JEV HN strain Sw/Mie/40/2004 leads to significant upregulation of the *SLC7A11* mRNA to levels comparable to *DDIT3* (Fig. 5a). In contrast, increasing titers of JEV lead to

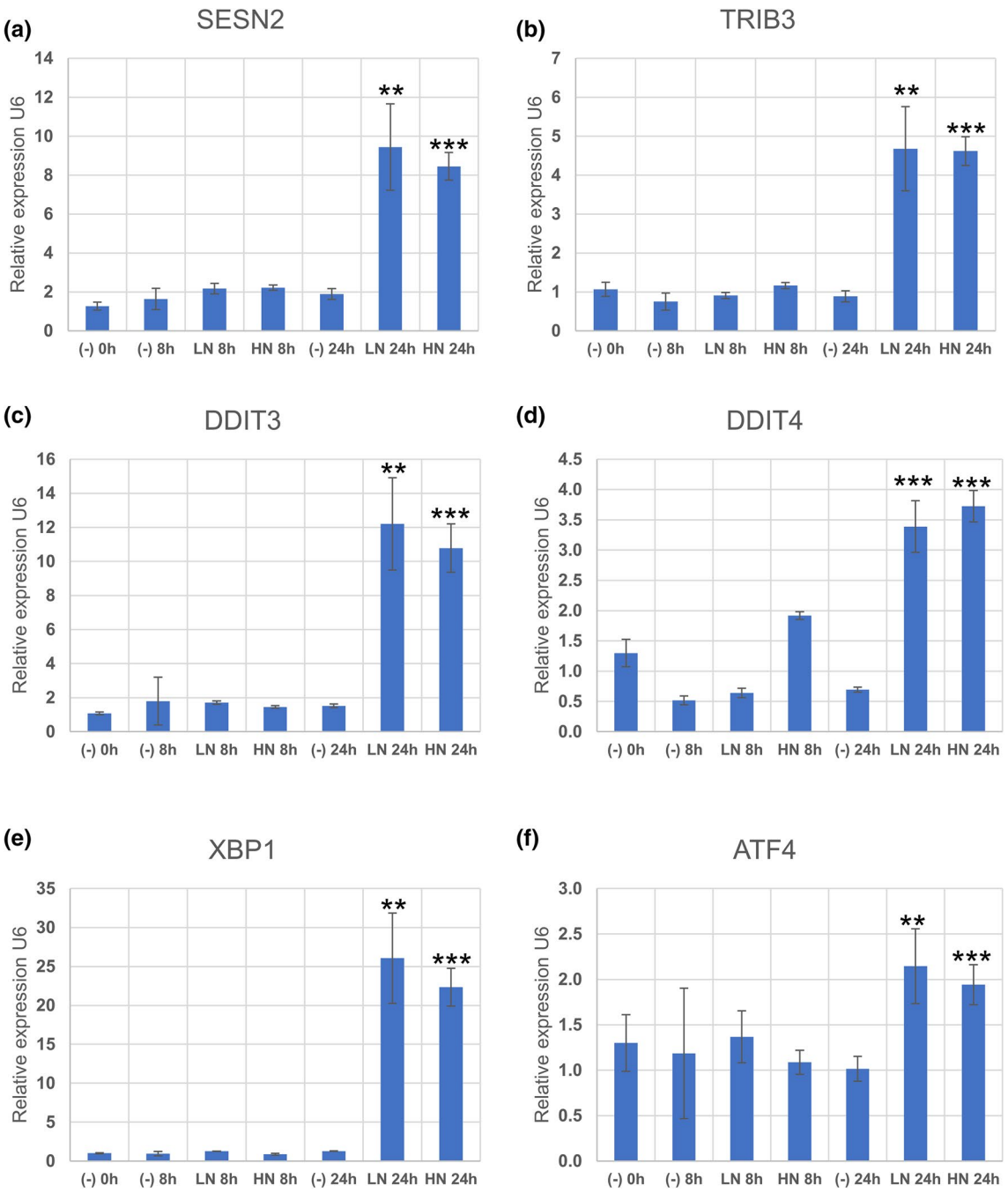

Fig. 2 Sestrin 2 and ER stress-signaling transcripts are significantly deregulated in JEV-infected neurons. The endoplasmic reticulum stress-signaling transcripts, *SESN2*, *TRIB3*, *DDIT3*, *DDIT4*, *XBP1*, and *ATF4* (**a**–**f**), were examined by specific SYBR green qPCR assays following mock or JEV infection with low or high neurovirulence strains (MOI 25) of SH-SY5Y neuroblastoma cells at the indicated time points. The relative mRNA levels to the endogenous control *U6* were measured by qPCR and presented as the fold change compared to mock-infected control cells at 0 h. The standard deviation was calculated from four biological replicates at each indicated time point. (−) 0 h: mock-infected 0 h; (−) 8 h: mock-infected 8 h; LN 8 h: JEV LN-infected 8 h; HN 8 h: JEV HN-infected 8 h; (−) 24 h: mock-infected 24 h; LN 24 h: JEV LN-infected 24 h; HN 24 h: JEV HN-infected 24 h. Statistical significance was evaluated at each time point relative to transcripts levels of uninfected SH-SY5Y cells at 0 h. $^{*}P<0.05$; $^{**}P<0.01$; $^{***}P<0.001$

upregulation at 24 hpi in HEK293T cells; however, the relative levels were lower than detected in neuronal cells and, also, *SLC7A11* upregulation appeared to precede increases of *DDIT3* mRNA at lower MOIs (see MOI1 in Fig. 5b). Immunofluorescence indicated that HEK293T cells infected with higher MOIs of JEV had high numbers of fluorescent

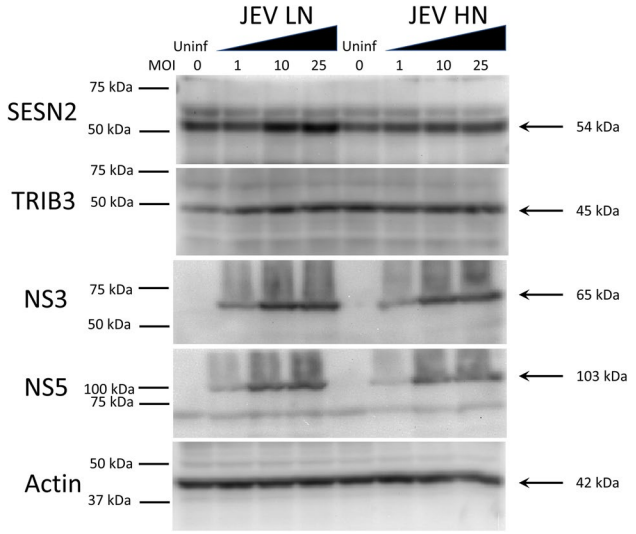

Fig. 3 SESN2 protein expression is deregulated in JEV-infected SH-SY5Y cells. Immunoblot analysis of SH-SY5Y mock-infected and infected with increasing MOIs (1, 10 and 25) of JEV LN and HN strains 24 hpi. Molecular weights are indicated in kiloDaltons (kDa) relative to molecular weight markers on the left and the predicted sizes of the specific proteins are indicated on the right. Uninfected cells served as mock controls

foci demonstrating human embryonic kidney cells are susceptible to JEV infection (Supplementary Fig. 5).

Discussion

In this study, we report for the first time the deregulation of the antioxidant SESN2 in human neuroblastoma cells in vitro following flavivirus (JEV and ZIKV) infection. Sestrins are a family of evolutionarily conserved stress-response proteins which are transcriptionally regulated by p53 and forkhead transcription factors and that are cytoprotective by exerting an antioxidant oxidoreductase activity in vitro that counteracts oxidative stress [17]. SESN2 plays two separable and independent functions: regulation of ROS and autophagy via mTORC1 regulation [45] and, thus, has emerged as a therapeutic target for diverse diseases, including malignancy, metabolic disorders, cardiovascular, and neurodegenerative diseases [45]. ER stress can occur when unfolded proteins accumulate, such as during flavivirus replication within the ER lumen [46]. In JEV infection, Su and co-workers previously identified upregulation of the transcription factor DDIT3 (CHOP) following induction of the UPR following ER stress [46]. Sharma and colleagues have also previously shown that depletion of XBP1 during JEV infection prevented the induction of autophagy and neuronal cell death showing its essential role in the autophagic process during flavivirus infection [47].

Interestingly, SESN2 protein levels have been found to be higher in patients suffering from Alzheimer's disease and PD [48–50] suggesting a role in neurotoxicity and that SESN2 malfunction may be associated with neuropathology. The link between elevated SESN2 and PD is particularly intriguing in the context of JEV infection as one of the distinct neurological sequelae associated with JEV is a Parkinsonian-like phenotype [51]. We suggest that studies should be performed to examine the levels of SESN2 in post-mortem sections to determine whether flaviviral antigens and SESN2 co-localize in vivo and specifically within the substantia nigra dopamine-producing neurons [51, 52]. In addition, SESN2 has been shown to promote Parkin-induced mitophagy—a process whereby mitochondria are selectively degraded by autophagy, which is essential for maintenance of undamaged mitochondria and the reduction of inflammasome activation [53]. Mutations in the *Parkin* gene have also been previously associated with autosomal recessive familial PD [54]. *SESN2* expression has also been found to be deregulated in the brain of HIV-associated neuronal disorders causing increased oxidative stress [48]. In post-mortem brain sections from cases of HIV-associated neurodegeneration (HAND), redistribution of SESN2 immunoreactivity from the neuropil (the unmyelinated axonal and dendritic processes) to the soma (the neuronal cell body) was evident [48]. The authors interpreted this redistribution of SENS2 to the neuronal soma to be the result of the increased oxidative stress occurring in the context of HIV infection and that neuronal stress is implicated in the pathophysiology of HAND. Whether a comparable redistribution of SESN2 to the soma is seen in the brains of mouse and rat models of flavivirus encephalopathy or in the post-mortem sections of human cases is unknown.

We show in this study that the *tribbles 3 pseudokinase* (*TRIB3*) mRNA was also significantly upregulated in both JEV and ZIKV infection of neuroblastoma cells in vitro. TRIB3 has been previously implicated in hepatitis C virus (HCV) replication, an hepatotropic flavivirus, as RNA-Seq studies showed TRIB3 to be upregulated [55]. TRIB3 knockdown leads to elevated HCV replication and increased virally encoded proteins, whereas TRIB3 overexpression diminished viral replication. The available data suggest HCV hijacks TRIB3-Akt pathway to enable viral persistence and may contribute to chronic HCV infection [55]. It remains to be determined whether TRIB3 also plays a comparable role in the replication of mosquito-transmitted flaviviruses.

Recently, Mukherjee and colleagues employing a human neural stem cell (hNS1 cell line) model of JEV infection conducted an analysis of the host proteome response at 72 hpi [56]. Consistent with the findings in the present study of JEV infection at 24 hpi that ER UPR was the top GO term identified, Mukherjee identified signaling through all ER UPR pathway proteins (PERK, IRE-1, and ATF6 and

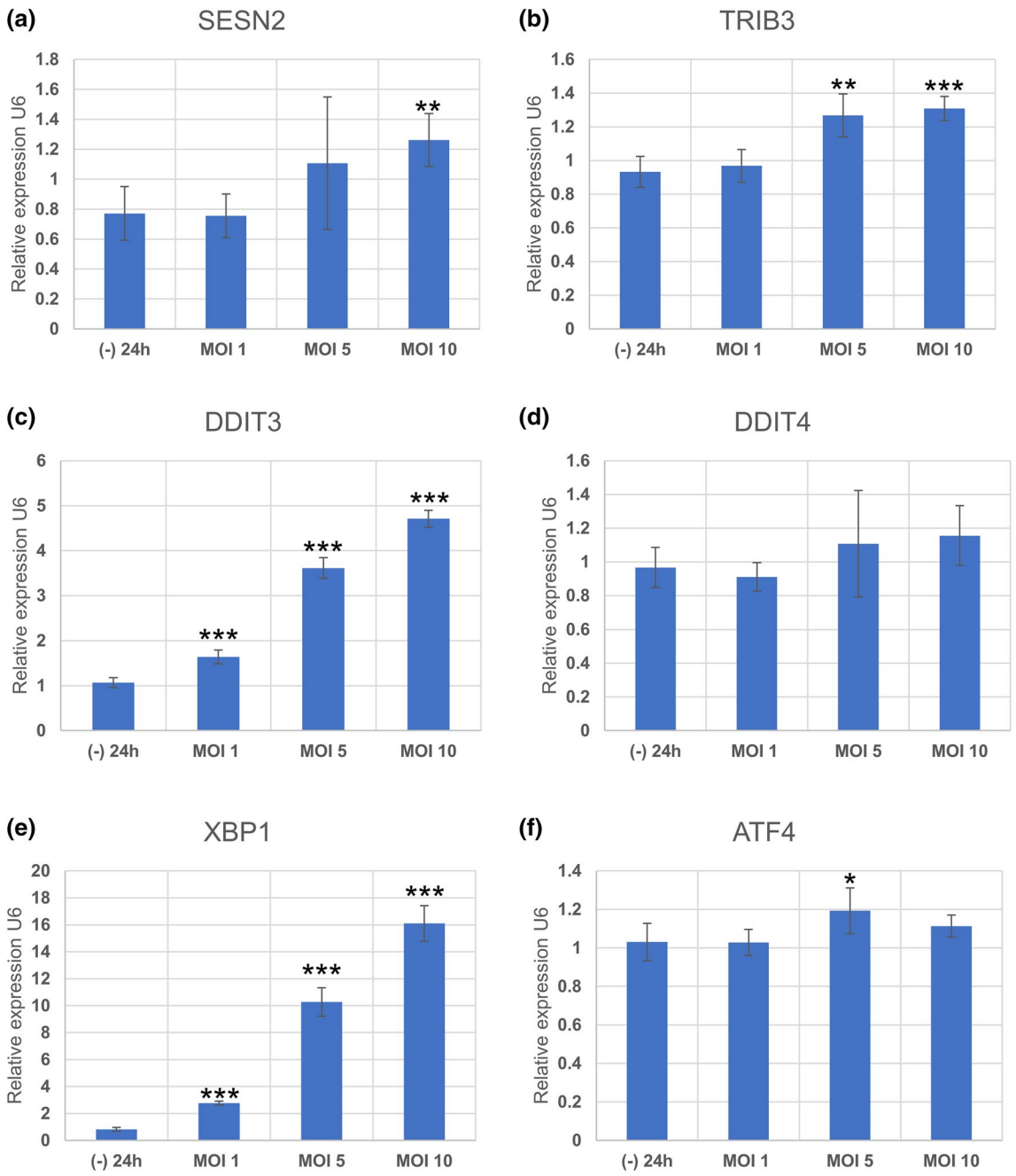

Fig. 4 ER stress-signaling transcripts are significantly deregulated in ZIKV-infected neurons. The endoplasmic reticulum stress-signaling transcripts, *SESN2*, *TRIB3*, *DDIT3*, *DDIT4*, *XBP1*, and *ATF4* (**a**–**f**), were examined by specific SYBR green qPCR assays following mock or ZIKV (prototype strain MR766) infection of SH-SY5Y neuroblastoma cells at 24 h with increasing MOIs (1, 5, and 10). The relative mRNA levels to the endogenous control *U6* were measured by qPCR and are presented as the fold change compared to mock-infected control cells at 24 h. The standard deviation was calculated from four biological replicates at each indicated time point. (−) 0 h: mock-infected 0 h; (−) 8 h: mock-infected 8 h; LN 8 h: JEV LN-infected 8 h; HN 8 h: JEV HN-infected 8 h; (−) 24 h: mock-infected 24 h; LN 24 h: JEV LN-infected 24 h; HN 24 h: JEV HN-infected 24 h. Statistical significance was evaluated relative to transcripts levels of uninfected SH-SY5Y cells at 24 h.*$P < 0.05$; **$P < 0.01$; ***$P < 0.001$

their downstream mediators) in hNS1 cells which trigger pro-apoptotic signals and ultimately caspase activation and cell death. GRP78, Calreticulin, Vimentin, PHB, hnRNPC, and Hyou1 were found by Mukherjee and co-workers to be significantly upregulated by JEV infection compared to mock-infected hNS1 cells 4 days post-infection. We note with interest that hypoxia-upregulated protein 1 (Hyou1) was also identified in the present study to be upregulated

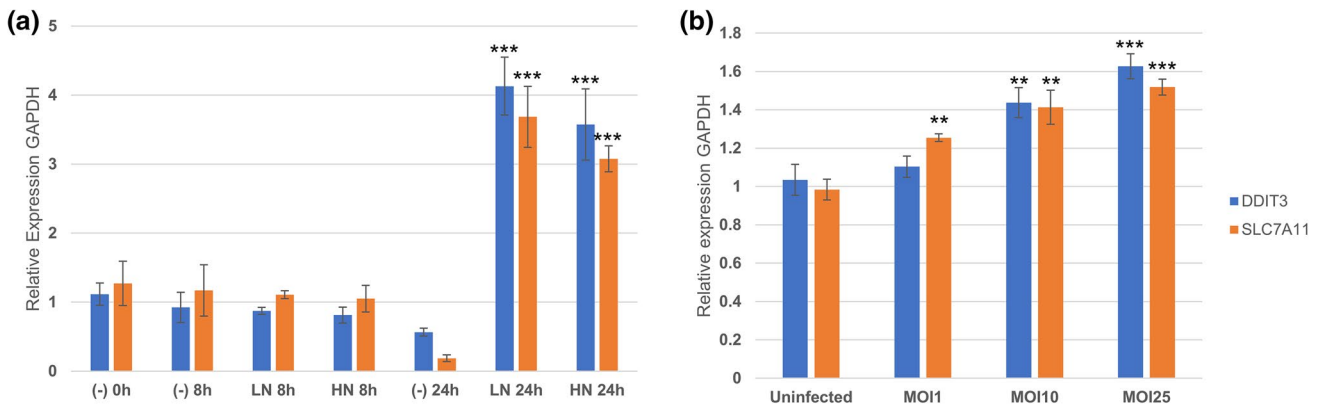

Fig. 5 The *SLC7A11* mRNA encoding the light chain of the xCT antiporter (system x_c^-) is deregulated in neuronal cells. **a** Relative expression of *SLC7A11* and *DDIT3* mRNA (the top ranked hit on the heat map in Fig. 1a) to GAPDH was examined by TaqMan qPCR following mock or JEV infection (MOI 25) with low or high neurovirulence strains of SH-SY5Y neuroblastoma cells at the indicated time points. Statistical significance was evaluated relative to transcripts levels of uninfected SH-SY5Y cells at 0 h.*$P<0.05$; **$P<0.01$; ***$P<0.001$. **b** Relative expression of *SLC7A11* and *DDIT3* was examined by TaqMan qPCR following mock or JEV infection with low or high neurovirulence strains of HEK293T cells at 24 hpi. Statistical significance was evaluated relative to transcripts levels of uninfected SH-SY5Y cells at 24 h.*$P<0.05$; **$P<0.01$; ***$P<0.001$

1 day post-infection of SH-SY5Y neuroblastoma cells (see Fig. 1c) and Hyou1 has previously been implicated in herpesvirus-associated inflammation and pathogenesis [57]. Further studies are required to determine whether Hyou1 plays a role in flavivirus-associated neuropathogenesis.

Interestingly, Tang and co-workers employing a ZIKV human neural progenitor cell (hNPC) model of infection also identified upregulation of *SESN2*, *TRIB3*, and *SLC7A11* transcripts following RNA-Seq analysis 3 days after infection with a low MOI (0.01) [58]. While this prior study focused on the increased cell death and cell-cycle dysregulation following ZIKV infection, it employed the same prototype strain (MR766), however, a different cell line and a later time point than the present study which suggests that sustained expression of *SESN2*, *TRIB3* and *SLC7A11* may be a general feature that occurs during flavivirus infection of neuronal-derived cells.

Glutamate excitotoxicity has been previously implicated in a number of neurological diseases, such as PD, Alzheimer's disease, multiple sclerosis, amyotrophic lateral sclerosis, and Huntington's disease [59]. System x_c^- activation results in the efflux of glutamate and the influx of cystine and represents the principal source of extracellular glutamate in certain regions of the brain [60], including the hippocampus and striatum where JEV antigen has been identified in post-mortem autopsies [8]. Hypothetically, in virus-induced encephalitis enhancement of the x_c^- antiporter activity may induce deleterious effects via release into the extracellular space of toxic quantities of glutamate; however, system x_c^- fulfills a dual role by providing cysteine (arising from the immediate reduction of the imported oxidized cystine) [61] and stimulating glutathione synthesis [62]. Our findings raise the possibility that system x_c^- is potentially implicated in the pathophysiology of JEV-induced neurodegeneration. The amino acid glutamate represents the principle activator of excitatory neurotransmitter receptors in mammalian central nervous systems and, therefore, the concentration of extracellular glutamate is maintained at extremely low levels in non-diseased states [63]. Increased activity of the extrasynaptic glutamatergic system has been associated with excitotoxic neuronal injury in several brain pathologies related to excitotoxicity, neurodegeneration, and neuroinflammation [63]. Neurodegenerative diseases are typified by both excitotoxicity and neuroinflammatory processes that ultimately leads to neuronal damage and subsequent death [60]. An emerging hypothesis in the study of glial, and other brain tumors, is that glutamate release is a self-preservation mechanism elicited by cancerous cells [61]. Upregulating the xCT antiporter (system x_c^-) leads to an increase in the uptake and the intracellular concentration of cystine, an essential amino acid, required for GSH synthesis, an antioxidant required for tumor proliferation and survival [62]. Whether an analogous scenario exists in flavivirus-infected neuronal cells with increased reactive oxygen species and ER stress necessitating increased GSH biosynthesis but coupled to the deleterious effects associated with increased glutamate excitotoxicity is suggested by the present work as we determined significantly increased *SLC7A11* and *SLC3A2* mRNA transcripts in JEV-infected neuroblastoma cells by RNA-Seq. Indeed, *SLC7A11* upregulation in HEK293T cells, while relative levels were decreased compared to the upregulation determined in SH-SY5Y cells, showed that this preceded the upregulation of the DNA damage response transcription factor *DDIT3* which was the most significantly deregulated

neuronal transcript in the RNA-Seq analysis. Several transcription factors that regulate xCT expression have been identified. The PI3K/Akt/GSK3β/eIF2α/ATF4 pathway has been recently shown to be implicated in increased xCT expression in the hippocampal region in neurological disorder [64]. ATF4 can bind to a number of amino acid response elements in the promoter of the specific light chain subunit of xCT (i.e., SLC7A11) resulting in elevated transcription of xCT. Our transcriptomic analysis and qPCR analysis showed ATF4 was also significantly upregulated in JEV-infected neuronal cells in vitro suggesting this may be the mechanism whereby increased *SLC7A11* expression occurs. Whether some of the neurological manifestations of JEV and other flaviviral-associated encephalitides are attributable to glutamate excitotoxicity arising from increased system x_c^- expression and glutamate excitotoxicity is unknown and warrants further study.

Acknowledgements We are extremely grateful to Dr. Tomohiko Takashi from the National Institute of Infectious Diseases, Tokyo for the kind gift of the JEV strains and to Dr. Takashi Kimura (Hokkaido University) for rabbit anti-JEV hyperimmune sera. This study was supported in part by a grant to Dr. Michael Carr from the Japanese Society for the Promotion of Science (JSPS/KAKENHI) of Japan (16K08803). This study was also supported in part by grants to Professor Hirofumi Sawa for Scientific Research on Innovative Areas from the Ministry of Education, Culture, Science, Sports and Technology (MEXT) of Japan (16H06429, 16H06431, 16K21723), grants from the Ministry of Education, Culture, Sports, Science and Technology; the Ministry of Health, Labour and Welfare, Japan (MEXT)/JSPS KAKENHI (16H05805).

Author contributions All authors contributed to the study design. MC performed the experiments and GG and AM performed the bioinformatic analyses. All authors contributed to data analysis and the writing and editing of the manuscript.

Compliance with ethical standards

Conflict of interest The authors declare that they have no conflicts of interest.

Research involving human participants or animals This article does not contain any study involving either human participants or animals performed by any of the authors.

References

1. Takayama J. Japanese encephalitis. WHO, 2015
2. Yin Z, Wang X, Li L, Li H, Zhang X, Li J, Ning G, Li F, Liang X, Gao L, Liang X, Li Y (2015) Neurological sequelae of hospitalized Japanese encephalitis cases in Gansu province, China. Am J Trop Med Hyg 92:1125–1129. https://doi.org/10.4269/ajtmh.14-0148
3. Ghosh D, Basu A (2009) Japanese encephalitis-a pathological and clinical perspective. PLoS Negl Trop Dis 3:e437. https://doi.org/10.1371/journal.pntd.0000437
4. Solomon T (2004) Flavivirus encephalitis. N Engl J Med 351:370–378. https://doi.org/10.1056/NEJMra030476
5. Campbell GL, Hills SL, Fischer M, Jacobson JA, Hoke CH, Hombach JM, Marfin AA, Solomon T, Tsai TF, Tsu VD, Ginsburg AS (2011) Estimated global incidence of Japanese encephalitis: a systematic review. Bull World Health Organ 89(766–774):774A–774E. https://doi.org/10.2471/BLT.10.085233
6. Myint KS, Kipar A, Jarman RG, Gibbons RV, Perng GC, Flanagan B, Mongkolsirichaikul D, Van Gessel Y, Solomon T (2014) Neuropathogenesis of Japanese encephalitis in a primate model. PLoS Negl Trop Dis 8:e2980. https://doi.org/10.1371/journal.pntd.0002980
7. Johnson RT, Burke DS, Elwell M, Leake CJ, Nisalak A, Hoke CH, Lorsomrudee W (1985) Japanese encephalitis: immunocytochemical studies of viral antigen and inflammatory cells in fatal cases. Ann Neurol 18:567–573. https://doi.org/10.1002/ana.410180510
8. Desai A, Shankar SK, Ravi V, Chandramuki A, Gourie-Devi M (1995) Japanese encephalitis virus antigen in the human brain and its topographic distribution. Acta Neuropathol 89:368–373
9. German AC, Myint KS, Mai NT, Pomeroy I, Phu NH, Tzartos J, Winter P, Collett J, Farrar J, Barrett A, Kipar A, Esiri MM, Solomon T (2006) A preliminary neuropathological study of Japanese encephalitis in humans and a mouse model. Trans R Soc Trop Med Hyg 100:1135–1145. https://doi.org/10.1016/j.trstmh.2006.02.008
10. Gupta N, Santhosh SR, Babu JP, Parida MM, Rao PV (2010) Chemokine profiling of Japanese encephalitis virus-infected mouse neuroblastoma cells by microarray and real-time RT-PCR: implication in neuropathogenesis. Virus Res 147:107–112. https://doi.org/10.1016/j.virusres.2009.10.018
11. Trottier MD Jr, Palian BM, Reiss CS (2005) VSV replication in neurons is inhibited by type I IFN at multiple stages of infection. Virology 333:215–225
12. Samuel MA, Diamond MS (2005) Alpha/beta interferon protects against lethal West Nile virus infection by restricting cellular tropism and enhancing neuronal survival. J Virol 79:13350–13361. https://doi.org/10.1128/JVI.79.21.13350-13361.2005
13. Daffis S, Samuel MA, Suthar MS, Gale M, Diamond MS (2008) Toll-like receptor 3 has a protective role against West Nile virus infection. J Virol 82:10349–10358. https://doi.org/10.1128/Jvi.00935-08
14. Cho H, Proll SC, Szretter KJ, Katze MG, Gale M, Diamond MS (2013) Differential innate immune response programs in neuronal subtypes determine susceptibility to infection in the brain by positive-stranded RNA viruses. Nat Med 19(4):458. https://doi.org/10.1038/nm.3108
15. Rosato PC, Leib DA (2015) Neuronal interferon signaling is required for protection against herpes simplex virus replication and pathogenesis. PLoS Pathog 11(1):456. https://doi.org/10.1371/journal.ppat.1005028
16. Budanov AV, Sablina AA, Feinstein E, Koonin EV, Chumakov PM (2004) Regeneration of peroxiredoxins by p53-regulated sestrins, homologs of bacterial AhpD. Science 304:596–600. https://doi.org/10.1126/science.1095569
17. Lee JH, Budanov AV, Park EJ, Birse R, Kim TE, Perkins GA, Ocorr K, Ellisman MH, Bodmer R, Bier E, Karin M (2010) Sestrin as a feedback inhibitor of TOR that prevents age-related pathologies. Science 327:1223–1228. https://doi.org/10.1126/science.1182228
18. Wullschleger S, Loewith R, Hall MN (2006) TOR signaling in growth and metabolism. Cell 124:471–484. https://doi.org/10.1016/j.cell.2006.01.016
19. Saxton RA, Sabatini DM (2017) mTOR signaling in growth, metabolism, and disease. Cell 168:960–976. https://doi.org/10.1016/j.cell.2017.02.004

20. Zoncu R, Efeyan A, Sabatini DM (2011) mTOR: from growth signal integration to cancer, diabetes and ageing. Nat Rev Mol Cell Biol 12:21–35. https://doi.org/10.1038/nrm3025
21. Lee JH, Budanov AV, Talukdar S, Park EJ, Park HL, Park HW, Bandyopadhyay G, Li N, Aghajan M, Jang I, Wolfe AM, Perkins GA, Ellisman MH, Bier E, Scadeng M, Foretz M, Viollet B, Olefsky J, Karin M (2012) Maintenance of metabolic homeostasis by Sestrin2 and Sestrin3. Cell Metab 16:311–321. https://doi.org/10.1016/j.cmet.2012.08.004
22. Budanov AV, Karin M (2008) p53 target genes Sestrin1 and Sestrin2 connect genotoxic stress and mTOR signaling. Cell 134:451–460. https://doi.org/10.1016/j.cell.2008.06.028
23. Maiuri MC, Malik SA, Morselli E, Kepp O, Criollo A, Mouchel PL, Carnuccio R, Kroemer G (2009) Stimulation of autophagy by the p53 target gene Sestrin2. Cell Cycle 8:1571–1576. https://doi.org/10.4161/cc.8.10.8498
24. Sanli T, Linher-Melville K, Tsakiridis T, Singh G (2012) Sestrin2 modulates AMPK subunit expression and its response to ionizing radiation in breast cancer cells. PLoS ONE 7(1):789. https://doi.org/10.1371/journal.pone.0032035
25. Budanov AV, Shoshani T, Faerman A, Zelin E, Kamer I, Kalinski H, Gorodin S, Fishman A, Chajut A, Einat P, Skaliter R, Gudkov AV, Chumakov PM, Feinstein E (2002) Identification of a novel stress-responsive gene Hi95 involved in regulation of cell viability. Oncogene 21:6017–6031. https://doi.org/10.1038/sj.onc.1205877
26. Kim MJ, Bae SH, Ryu JC, Kwon Y, Oh JH, Kwon J, Moon JS, Kim K, Miyawaki A, Lee MG, Shin J, Kim YS, Kim CH, Ryter SW, Choi AMK, Rhee SG, Ryu JH, Yoon JH (2016) SESN2/sestrin2 suppresses sepsis by inducing mitophagy and inhibiting NLRP3 activation in macrophages. Autophagy 12:1272–1291. https://doi.org/10.1080/15548627.2016.1183081
27. Mutz KO, Heilkenbrinker A, Lonne M, Walter JG, Stahl F (2013) Transcriptome analysis using next-generation sequencing. Curr Opin Biotech 24:22–30. https://doi.org/10.1016/j.copbio.2012.09.004
28. Yamaguchi Y, Nukui Y, Tajima S, Nerome R, Kato F, Watanabe H, Takasaki T, Kurane I (2011) An amino acid substitution (V3I) in the Japanese encephalitis virus NS4A protein increases its virulence in mice, but not its growth rate in vitro. J Gen Virol 92:1601–1606. https://doi.org/10.1099/vir.0.031237-0
29. Bray NL, Pimentel H, Melsted P, Pachter L (2016) Near-optimal probabilistic RNA-seq quantification. Nat Biotechnol 34:525–527. https://doi.org/10.1038/nbt.3519
30. Liao Y, Smyth GK, Shi W (2013) The Subread aligner: fast, accurate and scalable read mapping by seed-and-vote. Nucleic Acids Res 41:e108. https://doi.org/10.1093/nar/gkt214
31. Robinson MD, McCarthy DJ, Smyth GK (2010) edgeR: a Bioconductor package for differential expression analysis of digital gene expression data. Bioinformatics 26:139–140. https://doi.org/10.1093/bioinformatics/btp616
32. Love MI, Huber W, Anders S (2014) Moderated estimation of fold change and dispersion for RNA-seq data with DESeq2. Genome Biol. https://doi.org/10.1186/s13059-014-0550-8
33. Kimura T, Sasaki M, Okumura M, Kim E, Sawa H (2010) Flavivirus encephalitis: pathological aspects of mouse and other animal models. Vet Pathol 47:806–818. https://doi.org/10.1177/0300985810372507
34. Gidalevitz T, Stevens F, Argon Y (2013) Orchestration of secretory protein folding by ER chaperones. Biochim Biophys Acta 1833:2410–2424. https://doi.org/10.1016/j.bbamcr.2013.03.007
35. Lin D, Liang Y, Zheng D, Chen Y, Jing X, Lei M, Zeng Z, Zhou T, Wu X, Peng S, Huang K, Yang L, Xiao S, Liu J, Tao E (2018) Novel biomolecular information in rotenone-induced cellular model of Parkinson's disease. Gene 647:244–260. https://doi.org/10.1016/j.gene.2018.01.023
36. McLaughlin T, Falkowski M, Wang JJ, Zhang SX (2018) Molecular chaperone ERp29: a potential target for cellular protection in retinal and neurodegenerative diseases. Adv Exp Med Biol 1074:421–427. https://doi.org/10.1007/978-3-319-75402-4_52
37. Ma H, Dang Y, Wu Y, Jia G, Anaya E, Zhang J, Abraham S, Choi JG, Shi G, Qi L, Manjunath N, Wu H (2015) A CRISPR-based screen identifies genes essential for west-nile-virus-induced cell death. Cell Rep 12:673–683. https://doi.org/10.1016/j.celrep.2015.06.049
38. Hoshino T, Murao N, Namba T, Takehara M, Adachi H, Katsuno M, Sobue G, Matsushima T, Suzuki T, Mizushima T (2011) Suppression of Alzheimer's disease-related phenotypes by expression of heat shock protein 70 in mice. J Neurosci 31:5225–5234. https://doi.org/10.1523/JNEUROSCI.5478-10.2011
39. Slodzinski H, Moran LB, Michael GJ, Wang B, Novoselov S, Cheetham ME, Pearce RKB, Graeber MB (2009) Homocysteine-induced endoplasmic reticulum protein (Herp) is up-regulated in parkinsonian substantia nigra and present in the core of Lewy bodies. Clin Neuropathol 28:333–343. https://doi.org/10.2379/Npx08162
40. Eletto D, Chevet E, Argon Y, Appenzeller-Herzog C (2014) Redox controls UPR to control redox. J Cell Sci 127:3649–3658. https://doi.org/10.1242/jcs.153643
41. Jauhiainen A, Thomsen C, Strombom L, Grundevik P, Andersson C, Danielsson A, Andersson MK, Nerman O, Rorkvist L, Stahlberg A, Aman P (2012) Distinct cytoplasmic and nuclear functions of the stress induced protein DDIT3/CHOP/GADD153. PLoS ONE 7:e33208. https://doi.org/10.1371/journal.pone.0033208
42. Nerome R, Tajima S, Takasaki T, Yoshida T, Kotaki A, Lim CK, Ito M, Sugiyama A, Yamauchi A, Yano T, Kameyama T, Morishita I, Kuwayama M, Ogawa T, Sahara K, Ikegaya A, Kanda M, Hosoya Y, Itokazu K, Onishi H, Chiya S, Yoshida Y, Tabei Y, Katsuki K, Tabata K, Harada S, Kurane I (2007) Molecular epidemiological analyses of Japanese encephalitis virus isolates from swine in Japan from 2002 to 2004. J Gen Virol 88:2762–2768. https://doi.org/10.1099/vir.0.82941-0
43. Lewerenz J, Hewett SJ, Huang Y, Lambros M, Gout PW, Kalivas PW, Massie A, Smolders I, Methner A, Pergande M, Smith SB, Ganapathy V, Maher P (2013) The cystine/glutamate antiporter system x_c^- in health and disease: from molecular mechanisms to novel therapeutic opportunities. Antioxid Redox Sign 18:522–555. https://doi.org/10.1089/ars.2011.4391
44. Shin CS, Mishra P, Watrous JD, Carelli V, D'Aurelio M, Jain M, Chan DC (2017) The glutamate/cystine xCT antiporter antagonizes glutamine metabolism and reduces nutrient flexibility. Nat Commun. https://doi.org/10.1038/ncomms15074
45. Pasha M, Eid AH, Eid AA, Gorin Y, Munusamy S (2017) Sestrin2 as a novel biomarker and therapeutic target for various diseases. Oxid Med Cell Longev. https://doi.org/10.1155/2017/3296294
46. Su HL, Liao CL, Lin YL (2002) Japanese encephalitis virus infection initiates endoplasmic reticulum stress and an unfolded protein response. J Virol 76:4162–4171
47. Sharma M, Bhattacharyya S, Sharma KB, Chauhan S, Asthana S, Abdin MZ, Vrati S, Kalia M (2017) Japanese encephalitis virus activates autophagy through XBP1 and ATF6 ER stress sensors in neuronal cells. J Gen Virol 98:1027–1039. https://doi.org/10.1099/jgv.0.000792
48. Soontornniyomkij V, Soontornniyomkij B, Moore DJ, Gouaux B, Masliah E, Tung S, Vinters HV, Grant I, Achim CL (2012) Antioxidant sestrin-2 redistribution to neuronal soma in human immunodeficiency virus-associated neurocognitive disorders. J Neuroimmune Pharmacol 7:579–590. https://doi.org/10.1007/s11481-012-9357-0
49. Zhou D, Zhan C, Zhong Q, Li S (2013) Upregulation of sestrin-2 expression via P53 protects against 1-methyl-4-phenylpyridinium

(MPP+) neurotoxicity. J Mol Neurosci 51:967–975. https://doi.org/10.1007/s12031-013-0081-x
50. Rai N, Kumar R, Desai GR, Venugopalan G, Shekhar S, Chatterjee P, Tripathi M, Upadhyay AD, Dwivedi S, Dey AB, Dey S (2016) Relative alterations in blood-based levels of sestrin in alzheimer's disease and mild cognitive impairment patients. J Alzheimers Dis 54:1147–1155. https://doi.org/10.3233/JAD-160479
51. Pradhan S, Pandey N, Shashank S, Gupta RK, Mathur A (1999) Parkinsonism due to predominant involvement of substantia nigra in Japanese encephalitis. Neurology 53:1781–1786. https://doi.org/10.1212/Wnl.53.8.1781
52. Ogata A, Tashiro K (2000) Parkinsonism due to predominant involvement of substantia nigra in Japanese encephalitis. Neurology 55:602. https://doi.org/10.1212/Wnl.55.4.602
53. Kumar A, Shaha C (2018) SESN2 facilitates mitophagy by helping Parkin translocation through ULK1 mediated Beclin1 phosphorylation. Sci Rep 8(1):615. https://doi.org/10.1038/s41598-017-19102-2
54. Kitada T, Asakawa S, Hattori N, Matsumine H, Yamamura Y, Minoshima S, Yokochi M, Mizuno Y, Shimizu N (1998) Mutations in the parkin gene cause autosomal recessive juvenile parkinsonism. Nature 392:605–608
55. Tran SC, Pham TM, Nguyen LN, Park EM, Lim YS, Hwang SB (2016) Nonstructural 3 protein of hepatitis C virus modulates the tribbles homolog 3/AKT signaling pathway for persistent viral infection. J Virol 90:7231–7247. https://doi.org/10.1128/JVI.00326-16
56. Mukherjee S, Singh N, Sengupta N, Fatima M, Seth P, Mahadevan A, Shankar SK, Bhattacharyya A, Basu A (2017) Japanese encephalitis virus induces human neural stem/progenitor cell death by elevating GRP78, PHB and hnRNPC through ER stress. Cell Death Dis 8(1):e2556. https://doi.org/10.1038/cddis.2016.394
57. Giffin L, Yan F, Ben Major M, Damania B (2014) Modulation of kaposi's sarcoma-associated herpesvirus interleukin-6 function by hypoxia-upregulated protein 1. J Virol 88:9429–9441. https://doi.org/10.1128/Jvi.00511-14
58. Tang HL, Hammack C, Ogden SC, Wen ZX, Qian XY, Li YJ, Yao B, Shin J, Zhang FR, Lee EM, Christian KM, Didier RA, Jin P, Song HJ, Ming GL (2016) Zika virus infects human cortical neural progenitors and attenuates their growth. Cell Stem Cell 18:587–590. https://doi.org/10.1016/j.stem.2016.02.016
59. Zhou Y, Wang X, Tzingounis AV, Danbolt NC, Larsson HP (2014) EAAT2 (GLT-1; slc1a2) glutamate transporters reconstituted in liposomes argues against heteroexchange being substantially faster than net uptake. J Neurosci 34:13472–13485. https://doi.org/10.1523/JNEUROSCI.2282-14.2014
60. Nguyen D, Alavi MV, Kim KY, Kang T, Scott RT, Noh YH, Lindsey JD, Wissinger B, Ellisman MH, Weinreb RN, Perkins GA, Ju WK (2011) A new vicious cycle involving glutamate excitotoxicity, oxidative stress and mitochondrial dynamics. Cell Death Dis 2:e240. https://doi.org/10.1038/cddis.2011.117
61. de Groot J, Sontheimer H (2011) Glutamate and the biology of gliomas. Glia 59:1181–1189. https://doi.org/10.1002/glia.21113
62. Singh S, Khan AR, Gupta AK (2012) Role of glutathione in cancer pathophysiology and therapeutic interventions. J Exp Ther Oncol 9:303–316
63. Pal B (2018) Involvement of extrasynaptic glutamate in physiological and pathophysiological changes of neuronal excitability. Cell Mol Life Sci. https://doi.org/10.1007/s00018-018-2837-5
64. Lewerenz J, Baxter P, Kassubek R, Albrecht P, Van Liefferinge J, Westhoff MA, Halatsch ME, Karpel-Massler G, Meakin PJ, Hayes JD, Aronica E, Smolders I, Ludolph AC, Methner A, Conrad M, Massie A, Hardingham GE, Maher P (2014) Phosphoinositide 3-kinases upregulate system X_c^- via eukaryotic initiation factor 2 alpha and activating transcription factor 4—A pathway active in glioblastomas and epilepsy. Antioxid Redox Signal 20:2907–2922. https://doi.org/10.1089/ars.2013.5455